

Linear theory and violent relaxation in long-range systems: a test case

W. Ettoumi^{1,2} and M.-C. Firpo²

¹ Ecole Normale Supérieure de Cachan, 94235 Cachan, France

² Laboratoire de Physique des Plasmas CNRS-Ecole Polytechnique, 91128 Palaiseau cedex, France

E-mail: wabh.ettoumi@ens-cachan.fr

E-mail: marie-christine.firpo@lpp.polytechnique.fr

Abstract. In this article, several aspects of the dynamics of a toy model for long-range Hamiltonian systems are tackled focusing on linearly unstable unmagnetized (i.e. force-free) cold equilibria states of the Hamiltonian Mean Field (HMF). For special cases, exact finite- N linear growth rates have been exhibited, including, in some spatially inhomogeneous case, finite- N corrections. A random matrix approach is then proposed to estimate the finite- N growth rate for some random initial states. Within the continuous, $N \rightarrow \infty$, approach, the growth rates are finally derived without restricting to spatially homogeneous cases. All the numerical simulations show a very good agreement with the different theoretical predictions. Then, these linear results are used to discuss the large-time nonlinear evolution. A simple criterion is proposed to measure the ability of the system to undergo a violent relaxation that transports it in the vicinity of the equilibrium state within some linear e-folding times.

Submitted to: *J. Phys. A: Math. Gen.*

PACS numbers: 05.20.-y, 05.20.Dd, 05.45.-a

1. Introduction

The Hamiltonian Mean Field (HMF) model has become a well-known toy model to address the intricate relationships between dynamics and statistical mechanics of long-range interacting systems. It is defined by the following Hamiltonian

$$\mathcal{H} = \sum_{i=1}^N \frac{p_i^2}{2} + \frac{1}{2N} \sum_{i,j=1}^N [1 - \cos(\theta_i - \theta_j)], \quad (1)$$

where N is the number of particles, and θ_i and p_i denote respectively the position and momentum of the i^{th} particle. A useful collective quantity to introduce is the magnetization vector (M_x, M_y) with

$$M_x = \frac{1}{N} \sum_{i=1}^N \cos \theta_i \quad \text{and} \quad M_y = \frac{1}{N} \sum_{i=1}^N \sin \theta_i \quad (2)$$

The average energy per particle $U = \mathcal{H}/N$ reads then

$$U = \sum_{i=1}^N \frac{p_i^2}{2N} + \frac{1}{2} (1 - M^2), \quad (3)$$

where $M \equiv \sqrt{M_x^2 + M_y^2}$ denotes the modulus of the magnetization vector.

Recently, much interest has been devoted to the so-called quasi-stationary states (QSS) which are known to be responsible for the very slow convergence towards the statistical mechanics equilibrium predictions. Far from being difficult to generate, these QSS naturally emerge from waterbag initial distributions [1, 2]. It is also known that initial waterbag conditions in momenta, associated to zero or almost zero initial magnetization, induce the longest lasting QSS. However, when lowering towards zero the initial temperature of the particles, it is possible to exhibit waterbag momenta configurations with vanishing magnetization which converge exponentially towards the Boltzmann-Gibbs equilibrium. This calls for a linear theory approach.

Linear stability of the HMF model about unmagnetized equilibrium states has been up to now mostly studied within the Vlasov framework [3, 10], which assumes in particular an infinite number of particles. Moreover, to the authors' knowledge, the linear stability of spatially inhomogeneous, unmagnetized, equilibria has not been considered yet, even in the continuous Vlasov approach.

The motivation of the present study is then twofold: Firstly and mostly, one wishes to tackle the linear study of the unmagnetized cold HMF equilibria, within a finite- N , therefore exact, framework; secondly, the ensuing nonlinear dynamics is briefly addressed to show that the thermalization of cold unmagnetized HMF systems finely illustrates Lynden-Bell's concept of violent relaxation for long-range systems.

In Section 2, we shall establish the finite- N framework used for the linear stability derivation. In Section 3, we shall calculate the exact linear growth rates for two finite- N equilibria, both of zero temperature and zero magnetization, and compare them to numerical simulations. Section 4 is dedicated to a random matrix approach for

the calculation of non-deterministic symmetric initial states growth rates. Section 5 tackles the general case, including the spatially inhomogeneous ones by introducing a fluid approach based on Vlasov framework. Section 6 ends this study by discussing the connections between the linear features just derived and the HMF thermalization properties. The dynamics of the cold unmagnetized HMF model is proposed as a paradigm of violent relaxation.

2. Linear dynamics about cold unmagnetized finite- N equilibria

The equations of motion can straightforwardly be written from Equation (1) as

$$\forall k \in \{1, \dots, N\}, \begin{cases} \dot{\theta}_k = p_k \\ \dot{p}_k = \frac{1}{N} \sum_{i=1}^N \sin(\theta_i - \theta_k) \equiv F_k \end{cases} \quad (4)$$

Using Equation (2), the force acting on the particle k may be written as

$$F_k = M_y \cos \theta_k - M_x \sin \theta_k. \quad (5)$$

Let us consider unmagnetized finite- N equilibria, namely stationary states of the equations of motion (4), with $M_x = M_y = 0$. This amounts to have $p_k^* = 0$ and angles θ_k^* distributed in such a way that $M_x = M_y = 0$. Let us remark that, since the total momentum $P = \sum_{i=1}^N p_i$ is a constant of motion, the zero momentum equilibrium case considered here is just the cold (i.e. monokinetic) case for the special choice $P = 0$.

Let us perform the linear stability of this system. In that purpose, we write $\theta_k = \theta_k^* + \delta\theta_k$ and $p_k = \delta p_k$ where the asterisk denotes the unperturbed solution. At first order in $\delta\theta_k$, the force δF_k felt by the particle k verifies

$$\delta F_k = \frac{1}{N} \left[\cos \theta_k^* \sum_{i=1}^N \cos \theta_i^* \delta\theta_i + \sin \theta_k^* \sum_{i=1}^N \sin \theta_i^* \delta\theta_i \right]. \quad (6)$$

This yields the following linear system

$$\begin{bmatrix} \left\{ \delta\dot{\theta}_k \right\} \\ \left\{ \delta\dot{p}_k \right\} \end{bmatrix} = \begin{bmatrix} 0_N & I_N \\ A & 0_N \end{bmatrix} \begin{bmatrix} \left\{ \delta\theta_k \right\} \\ \left\{ \delta p_k \right\} \end{bmatrix} \quad (7)$$

where I_N is the $N \times N$ identity matrix and A a $N \times N$ matrix defined by

$$A_{i,j} = \frac{1}{N} \cos(\theta_i^* - \theta_j^*). \quad (8)$$

The stability depends on the eigenvalues $\{\lambda_k\}$ of the Jacobian matrix in Equation (7). Let us name it J . The eigenvalue problem can now be reduced to the unique study of A using the following transformation

$$J - \lambda I_{2N} = \begin{bmatrix} -\lambda I_N & 0_N \\ A & I_N \end{bmatrix} \cdot \begin{bmatrix} I_N & -\frac{1}{\lambda} I_N \\ 0_N & -\lambda I_N + \frac{1}{\lambda} A \end{bmatrix} \quad (9)$$

provided $\lambda \neq 0$. Hence,

$$\det(J - \lambda I_{2N}) = \det(-\lambda I_N) \det(-\lambda I_N + \frac{1}{\lambda} A) = (-1)^N \det(A - \lambda^2 I_N). \quad (10)$$

In other words, writing χ_M the characteristic polynomial of M , one has

$$\chi_J(\lambda) = (-1)^N \chi_A(\lambda^2) \quad (11)$$

This factorization allows us to focus only on the matrix A , and deduce the eigenvalues of the higher-order matrix J by taking the square root of A ones. We shall now study the case of two particular finite- N equilibria that advantageously simplify A .

3. Exact finite- N treatment for two special cold force-free equilibria

3.1. The quiet start case

Having in mind the computational plasma terminology, we define the so-called "quiet start" configuration as the equilibrium characterized by an equirepartition of the particles on the circle. It is here formally described by $\forall k, \theta_k^* = 2\pi k/N$, up to some constant phase, and $p_k^* = 0$. Using this definition in Equation (8), the matrix A immediately reduces to

$$A_{i,j} = \frac{1}{N} \cos\left(\frac{2\pi}{N}(i-j)\right). \quad (12)$$

We notice that we can rewrite the coefficients as

$$A_{i,j} = A_{(i-j) \bmod N}, \quad (13)$$

which makes evident that A is a circulant matrix. Using Equation (11), it can be easily shown that its eigenvalues $\{\lambda_k^2\}$ are expressed as

$$\lambda_k^2 = \sum_{j=1}^N A_j e^{2ijk\pi/N}. \quad (14)$$

Moreover, since A is real and symmetric, its eigenvalues are real, and one can identify the previous equation with its real part, yielding

$$\lambda_k^2 = \frac{1}{N} \sum_{j=1}^N \cos\left(\frac{2j\pi}{N}\right) \cos\left(\frac{2jk\pi}{N}\right). \quad (15)$$

This is just

$$\lambda_k^2 = \frac{1}{2} (\delta_{k,1} + \delta_{k,N-1}), \quad (16)$$

so that A has only one double non-zero eigenvalue equal to $1/2$. Using Equation (11) finally yields the expected growth rate γ_{QS} coming from the spatially homogeneous Vlasov linear theory [3] for the cold waterbag as

$$\gamma_{QS} = \sqrt{\lambda_1^2} = \frac{1}{\sqrt{2}}, \quad (17)$$

with no finite- N correction. In order to test the validity of this linear study, we performed numerical simulations based on a fourth-order symplectic integrator [5]. Starting from a quiet start configuration, every particle is moved by a uniformly randomized quantity $\epsilon \ll 2\pi/N$. As shown in Figure 1, the behaviour of the system

during the early times shows a very good agreement with the predicted exponential growth, and does not depend on the number of particles, which only changes the initial magnetization resulting from the perturbation.

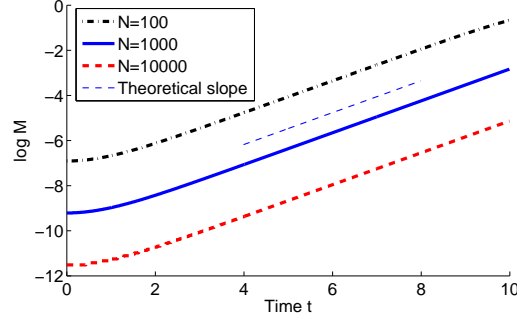


Figure 1. Numerical plot of the magnetization with respect to time. As predicted by Equation (17), the slope does not depend on the number of particles N , and is in very good agreement with the theoretical value of $1/\sqrt{2}$, plotted in thick dashed line.

3.2. Bi-clustered quiet start

The previous case involved a finite- N analog of a homogeneous Vlasov force-free equilibrium. We can construct another finite- N equilibrium with zero magnetization by uniformly distributing $N/2$ particles in a cluster of size $\Delta\theta$ centered on a given position, and by settling the positions of the $N/2$ remaining ones by rotating the first cluster by π with

$$\forall k \in \left\{1, \dots, \frac{N}{2}\right\}, \begin{cases} \theta_k^* = -\Delta\theta + \frac{4k\Delta\theta}{N} \\ \theta_{N/2+k}^* = \theta_k^* + \pi \\ p_k^* = 0 \end{cases} \quad (18)$$

Figure 2 shows an example of such a bi-cluster configuration. The same stability analysis

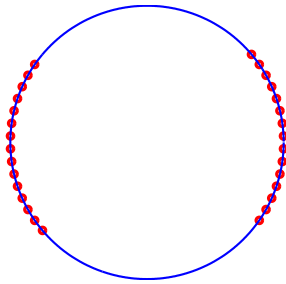


Figure 2. Plot of some finite- N bi-clustered equilibrium where each particle has a zero momentum and faces its symmetric on the circle, providing a zero magnetization.

as in the homogeneous quiet start case can be performed. However, one expects now the growth rate to depend on $\Delta\theta$, the clusters' size. Equation (11) is still valid, but

the matrix A is no longer circulant as it was in the simple quiet start case. A can be rewritten under the form

$$A = \begin{bmatrix} L & -L \\ -L & L \end{bmatrix}, \quad (19)$$

where L is a $N/2 \times N/2$ matrix with coefficients

$$L_{ij} = \frac{1}{N} \cos\left(\frac{4\Delta\theta}{N}(i-j)\right). \quad (20)$$

Therefore, the characteristic polynomial of A reads

$$\det(A - \lambda^2 I_N) = (-2\lambda^2)^{N/2} \det\left(L - \frac{\lambda^2}{2} I_{N/2}\right). \quad (21)$$

Or, equivalently,

$$\chi_A(\lambda^2) = (-2\lambda^2)^{N/2} \chi_L\left(\frac{\lambda^2}{2}\right) \quad (22)$$

This decomposition allows us to focus on the smaller matrix L . Unfortunately, L is not circulant either, but is a Toeplitz matrix. Indeed, one can write $L_{ij} = L_{|i-j|}$. A work performed by Treichler [6] showed that for a $m \times m$ Toeplitz matrix generated from the coefficients $t_k = \cos(k\omega)$, the only two non-zero eigenvalues are

$$\tilde{\nu}_{\pm}(m, \omega) = \frac{1}{2} \left(m \pm \frac{\sin(m\omega)}{\sin(\omega)} \right). \quad (23)$$

Equation (23) allows us to obtain the eigenvalues $\{\nu_k\}$ of the matrix L

$$\nu_{\pm} = \frac{1}{N} \tilde{\nu}_{\pm} \left(\frac{N}{2}, \frac{4\Delta\theta}{N} \right) = \frac{1}{4} \pm \frac{\sin(2\Delta\theta)}{2N \sin(4\Delta\theta/N)}. \quad (24)$$

Equations (11), (22) and (24) give the growth rate as

$$\gamma_{BCQS} = \sqrt{2\nu_+} = \sqrt{\frac{1}{2} + \frac{\sin(2\Delta\theta)}{N \sin(4\Delta\theta/N)}}, \quad (25)$$

that is, in the large N limit,

$$\gamma_{BCQS} = \frac{\sqrt{1 + \text{sinc}(2\Delta\theta)}}{\sqrt{2}}, \quad (26)$$

up to $\mathcal{O}(N^{-2})$ terms. Figure (3) shows the comparison between the numerically computed growth rates and the theoretical prediction of Equation (25). When $\Delta\theta = \pi/2$, particles are uniformly distributed on the circle as in the previous equilibrium and the growth rate is exactly $1/\sqrt{2}$ with no finite- N correction. Otherwise, the growth rate depends on the number of particles but we checked that the difference with the asymptotic result (26) is already very small for N above 10 particles.

We should note that in Reference [4], the authors diagonalize the matrix $T_{ij} = \cos(\theta_i - \theta_j)$ and give an analytic expression of its two non-zero eigenvalues. However, using their formula for a practical calculus requires the knowledge of an implicitly defined parameter ψ , which analytical calculation, in a finite- N context, is impossible, let alone some degenerate cases.

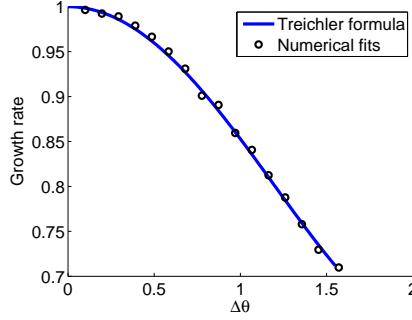


Figure 3. Plot of the growth rate as a function of $\Delta\theta$ for slightly perturbed bicluster initial configurations. The circles correspond to exponential fits from the numerically integrated magnetization, and the solid curve corresponds to Equation (25). Each numerical calculation has been performed with 1000 particles.

4. Extension to symmetric random initial configurations

In this section, we will only consider symmetric equilibria prepared to give $M = 0$ in the following way: we distribute $N/2$ particles at random on a partition of a given length and put the $N/2$ remaining particles by shifting the random ones by π . Using the appropriate indexation of particles (see (18)), the calculation of growth rates amounts to determine the largest eigenvalue of the $N/2 \times N/2$ matrix L defined by

$$\forall(i, j) \in \left\{1, \dots, \frac{N}{2}\right\}, \quad L_{ij} = \cos(\theta_i - \theta_j), \quad (27)$$

where the particle positions $\{\theta_i\}$ are distributed according to some $f_0(\theta)$, and where the $1/N$ normalization factor has been voluntarily omitted so that the coefficients' distribution do not depend on the number of particles. We used a method based on Random Matrix Theory to calculate the growth rate's expectation. When the random coefficients verify $\langle L_{ij} \rangle_{f_0} = \mu > 0$, an extension of Wigner's law [7] states that the largest eigenvalue is asymptotically approximated by

$$\nu = \frac{2}{N} \sum_{i,j}^{N/2} L_{ij} + \frac{\sigma^2}{\mu} + o\left(\frac{1}{\sqrt{N}}\right), \quad (28)$$

where $\sigma^2 = \langle L_{ij}^2 \rangle_{f_0}$. Since $\langle L_{ii} \rangle_{f_0} = 1$, Theorem 2 in Reference [7] states that ν has a normal distribution of expectation $1 + (N/2 - 1)\mu + \sigma^2/\mu$ and bounded finite variance $2\sigma^2$. Using Equations (11) and (22), one finds the mean squared growth rate as

$$\langle \lambda^2 \rangle = \frac{2}{N} \langle \nu \rangle = \frac{2}{N} \left[1 + \left(\frac{N}{2} - 1 \right) \mu + \frac{\sigma^2}{\mu} \right]. \quad (29)$$

The value of λ^2 is hence distributed according to a normal law of variance $8\sigma^2/N^2$ because of the $2/N$ rescaling factor. The expectation of the growth rate reads then

$$\langle \gamma \rangle = \mathcal{N}^{-1} \int_0^1 \sqrt{x} \exp \left[-\frac{N^2}{16\sigma^2} (x - \langle \lambda^2 \rangle)^2 \right] dx, \quad (30)$$

where \mathcal{N} is the normalization factor.

This approach simplifies the calculation of the growth rate, since no more effort in the diagonalization of matrix A has to be done. However, the most restrictive applicability condition of Equation (30) is the particular symmetry of the initial state, which allows the use of Equation (22). The conditions on the probability distribution of L_{ij} are not as limiting as the required symmetry of the initial state.

4.1. Random uniform bi-cluster

The equilibrium configuration generated by two symmetric waterbags of parameter $\Delta\theta$ yields a state topologically close to Eqs. (18). Therefore, we expect the growth rates for these random states to be close to the ones given in Equation (25). However, the latter Equation cannot be the asymptotic form of Equation (30) since the highest eigenvalue fluctuates around $1 + (N/2 - 1)\mu + \sigma^2/\mu$, which corresponds to the eigenvalue of the deterministic matrix $a_{ij} = \mu$ for $i \neq j$, $a_{ii} = 1$, that is completely different from the deterministic matrix L defined by Equation (20).

One needs to verify the applicability of Equation (28) before calculating the expectation of the growth rate with Equation (30). μ and σ^2 are accessible through the following formulae

$$\mu = \langle \cos(\theta_i - \theta_j) \rangle_{f_0} = \iint f_0(\theta_i) f_0(\theta_j) \cos(\theta_i - \theta_j) d\theta_i d\theta_j, \quad (31)$$

$$\sigma^2 + \mu^2 = \langle \cos^2(\theta_i - \theta_j) \rangle_{f_0} = \iint f_0(\theta_i) f_0(\theta_j) \cos^2(\theta_i - \theta_j) d\theta_i d\theta_j. \quad (32)$$

Writing $\chi(X)$ the characteristic function of the set X , the waterbag distribution of parameter $\Delta\theta$ has the probability density

$$f_0(\theta) = \frac{1}{2\Delta\theta} \chi([- \Delta\theta, \Delta\theta]). \quad (33)$$

Hence, we have

$$\mu = \text{sinc}^2(\Delta\theta), \quad (34)$$

$$\sigma^2 = \frac{1}{2} + \frac{\cos^2(\Delta\theta)}{4} \text{sinc}^2(\Delta\theta) - \mu^2. \quad (35)$$

Clearly, $\mu > 0$ for $\Delta\theta < \pi/2$ and σ^2 is finite, which means that Equation (30) holds. Figure (4) shows the numerical fits for randomized bi-clustered initial configurations and the theoretical mean value given by Equation (30). We also plotted the growth rate (25) corresponding to the deterministic bicluster to show that, as expected, its behaviour is close to the expectation of the random one for a wide range of $\Delta\theta$.

4.2. Random Gaussian bi-cluster

In this subsection we show another example of use of Equation (30) for a more difficult case. The particles are no longer distributed according to a waterbag density, but with a Gaussian one. We define $f_0(\theta)$ by

$$f_0(\theta) = \left[\sigma_\theta \sqrt{2\pi} \text{erf} \left(\frac{\pi}{2\sigma_\theta \sqrt{2}} \right) \right]^{-1} \exp \left(-\frac{\theta^2}{2\sigma_\theta^2} \right). \quad (36)$$

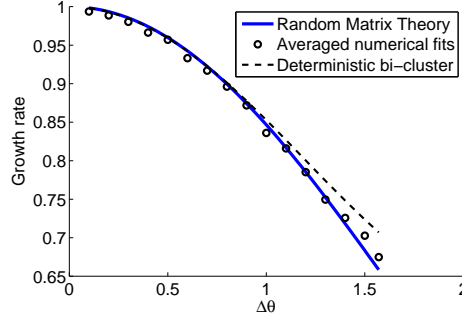


Figure 4. Plot of the growth rates from the uniformly randomized bicluster initial configuration with respect to $\Delta\theta$. The circles correspond to averaged exponential fits from the numerically integrated magnetization, the solid curve corresponds to Equation (30). The dashed curve corresponds to Equation (25). Each numerical calculation has been performed with 1000 particles, and each circle results from the average of 8 runs. We clearly see a very good agreement with the theoretical prediction.

The normalization factor has been calculated so that the particles are distributed on $[-\pi/2, \pi/2]$ with a standard deviation σ_θ^2 . Moreover,

$$\mu = \frac{e^{-\sigma_\theta^2}}{\text{erf}^2\left(\frac{\pi}{2\sigma_\theta\sqrt{2}}\right)} \left[\Re \left\{ \text{erf} \left(\frac{\pi - 2i\sigma_\theta^2}{2\sigma_\theta\sqrt{2}} \right) \right\} \right]^2 > 0 \quad (37)$$

$$\sigma^2 = \frac{1}{2} + \frac{e^{-4\sigma_\theta^2}}{8} \left[\text{erf}^2 \left(\frac{\pi}{2\sigma_\theta\sqrt{2}} \right) \right]^{-1} \left[2\Re \left(\text{erf} \left(\frac{\pi - 4i\sigma_\theta^2}{2\sigma_\theta\sqrt{2}} \right) \right) \right]^2 - \mu^2 \quad (38)$$

As shown on Figure (5), the agreement between the experimental average and the random matrix theory is very good.

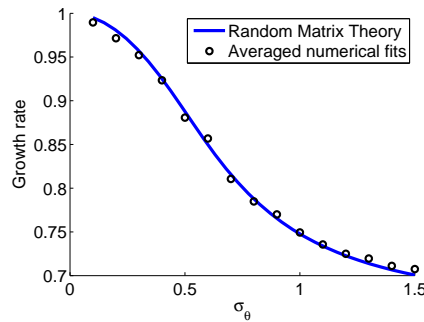


Figure 5. Plot of the growth rates as a function of σ_θ for the random Gaussian bicluster equilibria. The circles correspond to averaged exponential fits from the numerically integrated magnetization, while the curve corresponds to Equation (30). Each numerical calculation has been performed with 1000 particles, and each circle results from the average of 8 runs. Here again, the agreement with the random matrix theory prediction is very good.

In the general case, relaxing the symmetry assumption in the preparation of the finite- N equilibria yields a vanishing average value of the matrix elements of A

consistently with a vanishing magnetization. This prevents the application of the Theorem 2 of [7] and Equation (30) no longer holds. To overtake this difficulty, we now turn to the more usual continuous approach.

5. Linear theory within the continuous approach

Writing $f(\theta, p, t)$ the distribution function, one has the formal Vlasov equation

$$\frac{\partial f}{\partial t} + p \frac{\partial f}{\partial \theta} + E(\theta, t) \frac{\partial f}{\partial p} = 0. \quad (39)$$

One can define the density of particles $n(\theta, t)$ and the mean velocity field $v(\theta, t)$ through

$$n(\theta, t) = \int_{-\infty}^{+\infty} f(\theta, p, t) dp \quad \text{and} \quad v(\theta, t) = \frac{1}{n(\theta, t)} \int_{-\infty}^{+\infty} p f(\theta, p, t) dp. \quad (40)$$

The HMF force field $E(\theta, t)$ is then given by

$$E(\theta, t) = \int_{-\pi}^{\pi} \sin(\alpha - \theta) n(\alpha, t) d\alpha. \quad (41)$$

The early evolution of the cold HMF can be reduced to a fluid description. The hierarchy of the moments of the Vlasov equation can be stopped at the first order since the temperature vanishes. By taking the moment of order zero, one immediately obtains

$$\frac{\partial n}{\partial t} + \frac{\partial(nv)}{\partial \theta} = 0. \quad (42)$$

Multiplying Equation (39) by p and integrating over p , one has

$$\frac{\partial(nv)}{\partial t} + \int_{-\infty}^{+\infty} p^2 \frac{\partial f}{\partial \theta} dp - E(\theta, t)nv = 0. \quad (43)$$

Injecting Equation (42) in Equation (43) and dividing by n yields

$$\frac{\partial v}{\partial t} + v \frac{\partial v}{\partial \theta} - E(\theta, t) = 0, \quad (44)$$

in the cold case, for which the mean square of the momentum equals the square of the mean velocity. Considering the stationary solution given by some $n_0(\theta)$ yielding a zero magnetization, i.e. having a zero $m = 1$ Fourier component, and $v = 0$, one puts $v = \delta v(\theta) \exp(i\omega t)$ and $n = n_0(\theta) + \delta n(\theta) \exp(i\omega t)$ in Equations (41), (42) and (44). Expanding $\delta v(\theta)$ and $\delta n(\theta)$ in Fourier series, one obtains the linear system

$$\begin{aligned} i\omega \sum_m \delta n_m \exp(im\theta) + i \sum_m \sum_l (m+l) n_{0,m} \delta v_l \exp[i(m+l)\theta] &= 0, \\ i\omega \sum_m \delta v_m \exp(im\theta) + i\pi \sum_m \delta n_m (\delta_{-1,m} e^{-i\theta} - \delta_{1,m} e^{i\theta}) &= 0. \end{aligned}$$

This is

$$\omega \delta n_k + k \sum_m n_{0,m} \delta v_{k-m} = 0, \quad (45)$$

$$i\omega \delta v_{\pm 1} = \pm \frac{\pi}{\omega} \delta n_{\pm 1}, \quad (46)$$

and $\delta v_m = 0$ for $m \neq \pm 1$. This gives finally

$$\omega^2 \delta n_k + k\pi (n_{0,k-1} \delta n_1 - n_{0,k+1} \delta n_{-1}) = 0. \quad (47)$$

The dispersion relation is thus given by $\det M(\omega) = 0$, where M is generally an infinite matrix of elements

$$M_{k\ell} = \omega^2 \delta_{k,\ell} + k\pi (\delta_{\ell,1} n_{0,k-1} - \delta_{\ell,-1} n_{0,k+1}), \quad (48)$$

with $(k, \ell) \in \mathbb{Z}^2$.

Let us consider the finite-size $2N+1$ square matrix $\tilde{M}^{(N)}$, which coefficients coincide with M_{ij} , $\forall (i, j) \in \llbracket -N, N \rrbracket^2$. For $N = 1$, we have

$$\tilde{M}^{(1)} = \begin{bmatrix} \omega^2 + \pi n_{0,0} & 0 & -\pi n_{0,-2} \\ 0 & \omega^2 & 0 \\ -\pi n_{0,2} & 0 & \omega^2 + \pi n_{0,0} \end{bmatrix}. \quad (49)$$

The condition $\det \tilde{M} = 0$ is then fulfilled when

$$(\omega^2 + \pi n_{0,0})^2 = \pi^2 n_{0,2} n_{0,-2}, \quad (50)$$

but since $n(\theta, t)$ is real, $n_{0,-2} = \overline{n_{0,2}}$ where the bar denotes the complex conjugate. Therefore, one can take the square root in Equation (50), leading to

$$\omega_{\pm}^2 = -\pi n_{0,0} \pm \pi |n_{0,2}|. \quad (51)$$

It is then easy to show by recurrence that $\forall N$, $|\det \tilde{M}^{(N+1)}| = \omega^4 |\det \tilde{M}^{(N)}|$, so that Equation (51) gives the only non-vanishing roots to the general dispersion relation.

This allows to obtain the growth rate for the cold unmagnetized HMF in the infinite N limit as

$$\gamma = \frac{\sqrt{1 + 2\pi |n_{0,2}|}}{\sqrt{2}}, \quad (52)$$

where we used the fact that $n_0(\theta)$ is normalized giving $n_{0,0} = 1/2\pi$.

It is easy to check that the $N \rightarrow \infty$ growth rate (26) may be obtained from Equation (52) in the uniform bicluster configuration, for which $2\pi n_{0,2m} = \text{sinc}(2m\Delta\theta)$ and $n_{0,2m+1} = 0$, $\forall m \in \mathbb{Z}$. The formula (52) was successfully tested for a variety of spatially inhomogeneous equilibria with $M = 0$ (See the plots of the instantaneous growth rates \dot{M}/M with respect to time in Figure 6).

We shall now briefly discuss the large-time nonlinear features of the HMF model in the light of Lynden-Bell's picture of violent relaxation.

6. Final discussion on the cold HMF case : an example of violent relaxation

As two-body, collisional, relaxation timescales were far too large to account for the observed luminosity profiles of elliptical galaxies, the concept of violent relaxation was introduced by Lynden-Bell in his famous 1967 paper [8, 9]. Following this seminal study, there appears to be nowadays a common agreement on the scenario of the relaxation process for N -body long-range systems. It is supposed to be divided in two parts:

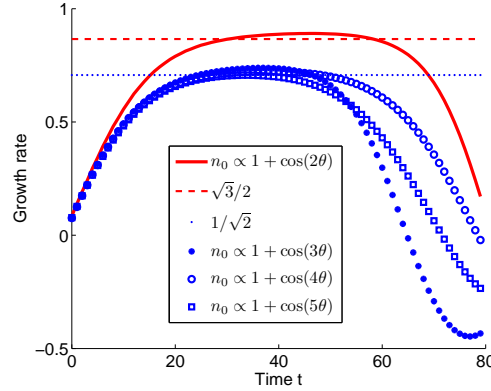


Figure 6. Plot of the numerical growth rate \dot{M}/M with respect to time for different initial equilibria. When the magnetization is almost exponential, \dot{M}/M is practically constant and matches the theoretical value given by Equation (52), represented by the horizontal lines. We clearly see that when the second harmonic of n_0 is zero, the growth rates are equal to $1/\sqrt{2}$ as in the homogeneous case. All the runs have been performed using 10^4 particles.

the properly speaking violent relaxation part, namely a rapid evolution of the system towards a quasi-stationary metastable state, followed by a much slower thermalization phase towards the state predicted by equilibrium statistical mechanics. The HMF model provides a simple yet nontrivial long-range system to consider this issue.

Extensive numerical studies of the HMF model are now available in the literature, mostly for two types of initial states: waterbag initial distribution functions in positions and momenta and Maxwellian initial distribution functions in momenta with possibly waterbag initial distribution functions for positions. Long-time discrepancies between time averaged observables and their ensemble predictions have been reported only with initial waterbag distributions in momenta, in connection with the emergence of so-called quasi-stationary states. Linear theory, mostly done within the Vlasov framework and for spatially homogeneous states, can be used as a guideline to discuss relaxation properties in the spirit of Lynden-Bell's picture. For instance, the spatially homogeneous cases with initial waterbag distributions in momenta are unstable with growth rates equal to $\sqrt{1/2 - 3T}$ where T is the initial temperature associated to the waterbag. Consequently, for $T > 1/6$ the system becomes linearly stable. This case corresponds to a density energy U equal to $7/12$ [3, 10]. This value happens to coincide with the energy threshold value above which pathological relaxation behaviours have been reported for spatially homogeneous, waterbag in momenta, initial distributions functions. There is then a simple, but apparently not explicitly formulated, manner to interpret the relaxation features observed in the HMF model: an efficient, rapid, convergence towards equilibrium statistical mechanics' predictions *requires* starting from the vicinity of an initially unstable equilibrium. Linear instability then naturally provides the violent relaxation phase. The cold case, on which we have just focused, illustrates well this scenario. Actually, large-time simulations show that the modulus of the magnetization,

for instance, quickly converges towards a saturated state with a value that is close to its ensemble prediction. It is interesting to note that similar observations have been reported for another long-range, mean-field, wave-particle Hamiltonian model starting with a cold beam of particles [12]. An heuristic way to explain this rapid convergence is through the comparison between the linear and nonlinear timescales available in the system. The linear timescale is obviously given by the e-folding time, namely by the inverse of the linear growth rate γ . The nonlinear timescale is the trapping time of the particles in the mean-field potential well, namely the inverse of the bounce frequency $\omega_b = M^{1/2}$. Nonlinear saturation takes place when both timescales balance, namely for $\gamma \sim \omega_b$. Therefore, one expects nonlinear saturation to take place close to equilibrium predictions provided that the linear growth rate is of the order of the ensemble average of the nonlinear frequency.

This is indeed the case for the cold system for which $U = 1/2$. According to equilibrium statistical dynamics [11], this gives $\langle M \rangle_\mu = \langle M \rangle_c = 1/\sqrt{\beta} \equiv \sqrt{T}$ where the inverse of the temperature is given implicitly by $I_1(\sqrt{\beta})/I_0(\sqrt{\beta}) = 1/\sqrt{\beta}$. Numerically, the ensemble average of the magnetization for the cold HMF is then $\langle M \rangle_c \simeq 0.62$ and the equilibrium temperature is $T \simeq 0.39$, which does yield $\gamma \sim \langle \omega_b \rangle_\mu$. Figure 7 shows that the cold unmagnetized HMF does experience a violent relaxation. The figure makes however apparent that that this phase is followed by a much slower thermalization phase that is needed for phase space sweeping and convergence towards equilibrium statistical predictions. Actually, in the early nonlinear saturation, the magnetization oscillates about 0.60, below the ensemble equilibrium value. The drift towards the equilibrium statistical predictions takes place on a much longer timescale than the violent relaxation timescale, which is the nonlinear saturation timescale of order γ^{-1} .

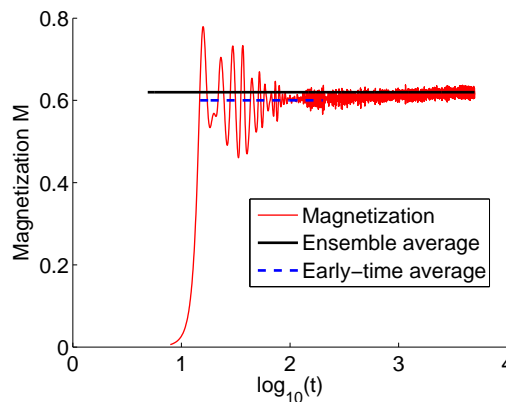


Figure 7. Time evolution of the magnetization starting from a gently perturbed homogeneous quiet start of the cold HMF.

- [1] Campa A *et al* 2009 *Phys. Rep.* **480** 57-159
- [2] Latora V, *et al* 2001 *Phys. Rev. E* **64** 056134
- [3] Antoni M and Ruffo S 1995, *Phys. Rev. E* **52** 2361-2374
- [4] Barre J, *et al* 2008, *Eur. Phys. J. B* **29** 577-591
- [5] Yoshida H, 1990 *Phys. Lett. 1* **150** 262-268

- [6] Treichler J R 1977, Ph.D. Dissertation, Stanford University
- [7] Füredi Z. and Komlós J. 1989 *Combinatorica* **1** 233-241.
- [8] Lynden-Bell D 1967 MNRAS **136** 101
- [9] White S D M in *Gravitational Dynamics*, Proc. 36th Herstmonceux Conference, ed O. Lahav *et al*, Cambridge University Press, Cambridge. p121
- [10] Yamaguchi Y *et al* 2006, *Physica A* **337**, 36
- [11] Rocha Filho T M *et al* 2009, *J. Phys. A: Math. Theor.* **42**, 165001
- [12] Firpo M C *et al* 2006, *Phys. Plasmas* **13** 122302 (2006).